URSI GASS 2021, Rome, Italy, 28 August - 4 September 2021

Assessing the measurability of perturbations in electron velocity distribution caused by nonlinear interaction with chorus subpackets

Miroslav Hanzelka*(1)(2), Ondřej Santolík(1)(2), Yoshiharu Omura(3), and Ivana Kolmašová(1)(2)
(1) Department of Space Physics, Institute of Atmospheric Physics, Czech Academy of Sciences, Prague, Czech Republic
(2) Faculty of Mathematics and Physics, Charles University, Prague, Czech Republic
(3) Research Institute for Sustainable Humanosphere, Kyoto University, Uji, Japan

Abstract

In this paper, we present a simulation of perturbations in the electron velocity distribution caused by the nonlinear resonant interaction with chorus emissions. Chorus is a whistler-mode electromagnetic wave phenomenon commonly observed in the Earth's magnetosphere. Through nonlinear cyclotron resonance, chorus scatters energetic electrons in kinetic energy and pitch angle and thus contributes to the formation of relativistic electron populations in the outer radiation belt. We model the chorus wavefield using the nonlinear growth theory and we run a test particle simulation to reconstruct the time evolution of electron velocity distributions at the equator. We further analyze the magnitude of perturbations in the distribution to evaluate the particle counts necessary for statistically significant measurements, and we compare these with the expected counts on the PEACE HEEA electron analyzers mounted on the Cluster spacecraft. It is shown that the resolution of these analyzers is not sufficient to detect the perturbations, thus explaining the lack of experimental evidence for the studied nonlinear effects on electron populations. However, with a dedicated experiment using the state-of-the-art technology, observations of these perturbations should be possible.

1 Introduction

The chorus electromagnetic emissions are a class of whistler-mode waves that occur naturally in the Earth's magnetosphere [1]. They are recognized as an important driver of electron acceleration in the outer radiation belt and are responsible for the production of relativistic electrons [2]. The electrons interact with counter-streaming whistler-mode waves through Doppler-shifted cyclotron resonance. The energy of the resonant particles ranges typically from about 1 keV to 100 keV for the lower frequency band of 0.1–0.5 Ω_e, where Ω_e denotes the local angular electron gyrofrequency [3]. In this frequency range, the emissions often exhibit highly structured spectra consisting of coherent, high-amplitude discrete elements with rising or falling frequencies. Based on observational evidence and theoretical investigations, the chorus wave elements are known to be formed around the magnetic equator and to propagate bidirectionally to higher latitudes, approximately following the magnetic field lines [4, 5]. Observations of the Cluster and Van Allen Probes spacecraft missions revealed a fine structure of chorus emissions with short wave subpackets within each element [6].

Several theories have been proposed to explain the formation of chorus emissions. The initial growth stage is well described by the linear growth theory. In the second stage, whistler-mode waves start entrapping increasing numbers of resonant electrons, forming a phase space hole and disturbing thus the gyrotropy of the electron distribution, which causes the formation of resonant currents [7]. The resonant current modifies the dispersion properties of the wave and results in an enhanced, nonlinear amplitude growth, and in a drifting wave frequency [8]. Other approaches replace the electromagnetic hole by a step function in the parallel velocity distribution function, which then serves as the energy source for the nonlinear growth [9]. However, no such features have been observed experimentally. Moreover, no theoretical approach so far has explained the formation of the subpackets within chorus elements. The presence of subpackets modifies the effectivity of electron acceleration, supporting thus the need for a better understanding of the fine structure of chorus.

Particle analyzers on satellites orbiting in the Earth's magnetosphere have so far not been successful in capturing the above described structures in the electron velocity distribution that might elucidate the subpacket formation process. In this article we study the perturbations to the hot electron distribution by means of test particle simulations on the background of a fixed chorus wave field. We conclude that the pitch angle resolution of electron analyzers carried by currently or recently operating satellites is insufficient to observe any of these stripes in their entirety. As it turns out, the most crucial deficiency comes from low particle counts, leading to the need of higher geometric factors of particle analyzers, in order to enable experimental confirmation of nonlinear effects of chorus on electron distributions.

2 Methods

To obtain the electromagnetic field of a parallel propagating chorus element with a rising frequency, we solved a system of differential equations describing the evolution of the amplitude of magnetic field fluctuations B_w and the angular wave frequency ω in the chorus source region. Next, we used transport equations to propagate the wave in one spatial dimension h along the magnetic field line. The method is based on the concept of antenna radiation from the resonant current and the modified chorus equations of the nonlinear growth theory, as described in [10]. The simulated chorus element features a realistic subpacket structure with an irregular growth of the wave frequency and with an upstream shift of the source region – these properties have been observed in numerical simulations and in spacecraft measurements [11, 5]. The frequency of the modeled element grows from $0.2\,\Omega_\mathrm{e0}$ to $0.5\,\Omega_\mathrm{e0}$, where Ω_e0 is the equatorial angular gyrofrequency. The time duration of the chorus element at the equator is about 340 ms. The ratio of plasma frequency to the equatorial gyrofrequency was set to $\omega_\mathrm{pe}/\Omega_\mathrm{e0} = 7$.

In the next step, the just described chorus wavefield is utilized in a test particle simulation. In order to obtain a very precise velocity distribution at a given point in space and time, we use the backward-in-time simulation method. In this approach, the equation of motion for electrons in an electromagnetic field is solved from a fixed final point (after the interaction with chorus) to an arbitrary initial point at which the wavefield disappears. The phase space densities corresponding to the velocity of electrons at the end of the simulation are mapped to the fixed final point with the use of Liouville's theorem. Therefore, if we know the initial, unperturbed distribution at all points along the magnetic field line and if we choose the velocities of electrons so that we cover uniformly the velocity space at the final point, we can obtain the phase space density of the electron distribution after the interaction with a chorus wave.

We sampled the parallel velocities in the range $v_\parallel \in (-0.5\,c, 0.0\,c)$ with 256 points, perpendicular velocities in the range $v_\perp \in (0.0\,c, 1.0\,c)$ with 256 points, and gyrophases $\varphi \in [0, 2\pi)$ with 64 points (particles with initial velocities larger than c are excluded from the sample). The test particles were advanced back in time by the volume preserving Boris algorithm. Effects of the mirror force on electrons were included through additional perpendicular components of the background magnetic field. The wave phase was bilinearly interpolated from a grid with $\Delta h = 1\,c\Omega_\mathrm{e0}^{-1}$, $\Delta t = 4\,\Omega_\mathrm{e0}^{-1}$ to the position of the particle.

Since the phase space density is supposed to be preserved in our physical system, the initial velocity distribution function must evolve adiabatically along field lines. We chose a distribution which is bi-Maxwellian in relativistic velocities $u_\parallel$, $u_\perp$. The distribution in the particle phases φ is set to be uniform. The choice of input parameters common to all simulation runs is the following: $\omega_\mathrm{phe} = 0.3\,\Omega_\mathrm{e0}$ (i.e. the equatorial hot electron density is $N_\mathrm{he,eq} = \omega_\mathrm{phe}^2 m\varepsilon_0/e^2$), relativistic parallel thermal velocity $U_{\parallel\mathrm{eq}} = 0.12\,c$, and relativistic perpendicular thermal velocity $U_{\perp\mathrm{eq}} = 0.25\,c$. The background magnetic field is assumed to be dipolar with equatorial strength at the Earth's surface of $3.1\cdot10^{-5}\,\mathrm{T}$, and the particles are propagating on the L-shell with $L = 4.5$. The corresponding equatorial electron gyrofrequency evaluates to $\Omega_\mathrm{e0} = 5.98\cdot10^4\,\mathrm{s}^{-1}$. These parameters and velocity distribution function are the same as in the equations of the nonlinear growth theory [10] used for the wave simulation.

3 Results

Using the test particle simulation method and input parameters described in the previous section, we analyzed the state of the electron velocity distribution function after the interaction with the entire chorus element wavefield. The time step is chosen to be a fixed value that is always below $2\pi\cdot0.02\Omega_\mathrm{e}^{-1}(h)$ along all trajectories, where $\Omega_\mathrm{e}(h)$ is the local electron gyrofrequency at a distance h from the magnetic equator. We set the final point to $h_\mathrm{f} = 0\,c\Omega_\mathrm{e0}^{-1}$, $t_\mathrm{f} = 21000\,\Omega_\mathrm{e0}^{-1} \approx 350\,\mathrm{ms}$, which is right after the end of the last subpacket at the equator.

During the resonant interaction, an electromagnetic hole forms in the $(\zeta, v_\parallel)$ space, where ζ is the angle between the wave magnetic field vector and the perpendicular particle velocity vector (the parallel resonance velocity is defined as $V_\mathrm{R} = (\omega - \Omega_e/\gamma)/k$, where γ is the Lorentz factor and k is the wave number). Particles trapped in the hole are transported to lower parallel velocities, while resonant particles that flow around the hole increase their parallel velocity. For a highly anisotropic distribution, this translates to an increase of the pitch angle $\alpha = \arctan(v_\parallel/v_\perp)$ and the kinetic energy E_k for trapped particles, and a decrease of α and E_k for untrapped particles. After integrating over gyrophases, we obtain a 2D velocity distribution where the hole is not apparent anymore, and the perturbed part of the distribution appears as a stripe along the relativistic resonance velocity curve. Interaction with each subpacket creates a new stripe at lower velocities, resulting in the perturbation depicted in Figure 1a.

Since the measuring capabilities of electron analyzers on spacecraft are usually restricted to recording the absolute number (count) of captured particles as a function of their kinetic energy and pitch angles, we should rather inspect the perturbations of the electron distribution using these variables. Moreover, the aforementioned simulation results represent the distribution at a single instant in time, while spacecraft particle analyzers typically require tens to hundreds of milliseconds to sweep through the relevant range of electron energies.

The first step in this measurability analysis is to determine the time interval and the range of energies and pitch angles

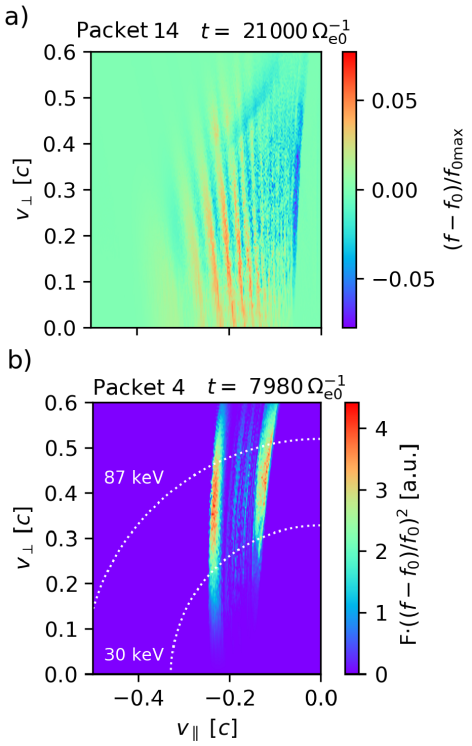

Figure 1. a) Perturbations of electron velocity distribution after the interaction with one chorus element, simulation starting at point $t = 21000\,\Omega_{e0}^{-1}$, $h = 0\,c\Omega_{e0}^{-1}$. Normalized difference between perturbed and initial 2D distributions shows the overlapping of stripes (each created through resonance with a single subpacket) and mixing of phase space densities, leading to a distortion of the stripe structure. b) The product of the differential flux and the inverse value of required particle count for the case of interaction with the fourth subpacket, given in arbitrary units. White dotted lines show the ideal energy range for measurements.

in which we observe large phase space density perturbations and, at the same time, large differential particle fluxes. If we assume the number N of particles measured in each energy-angle bin to be Poisson distributed, then the statistical uncertainty of the measurement can be represented by the relative standard deviation $1/\sqrt{N}$. So, in order to make the measurement of a density perturbation significant at the one-sigma level, we need at least $N_{C,req} = (f_0/(f - f_0))^2$ particles in each bin. The values of the differential electron flux F, which are proportional to the expected particle counts $N_{C,exp}$, have a maximum at about $v_\parallel = 0$, $v_\perp = 0.35c$. However, we need also need to look at the relative perturbations of the phase space density to minimize $N_{C,req}$. The quantity we use to determine the most suitable phase space region for measurements is $F/N_{C,req} \propto N_{C,exp}/N_{C,req}$. By looking at the state of the perturbed distribution after interaction with each subpacket, we determined that the highest values of $F/N_{C,req}$ are found between subpackets 4 and 7. A plot of $F/N_{C,req}$ is presented in Figure 1b (normalized to its maximum value) for the case of the fourth subpacket.

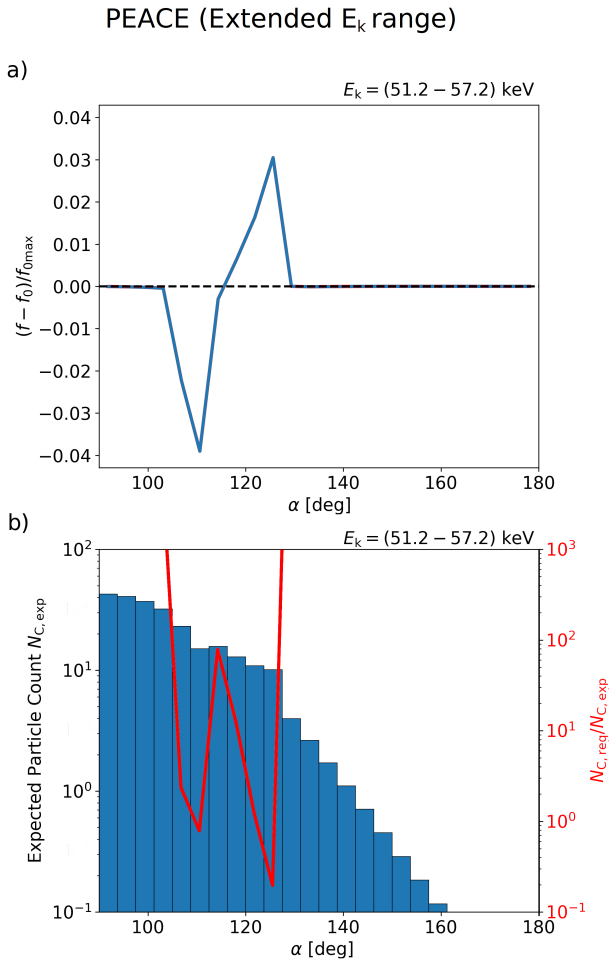

Figure 2. 1D pitch angle distribution and particle counts, based on the PEACE HEEA instrument with a hypothetical extension of its energy range and a modified operation mode. a) Normalized difference between the perturbed and the initial pitch angle distribution. Linear steps in pitch angle are chosen to match the polar angle resolution of the PEACE HEEA analyzers. b) Expected particle counts and the ratio of required (to reach one-sigma significance level) and expected counts.

In the second step, we tried to compare the size and magnitude of the simulated perturbations with the resolution of an actual spacecraft instrument. As an example we took the PEACE HEEA (High Energy Electron Analyzer) particle analyzer on the Cluster spacecraft [12]. The HEEA is a top-hat electron spectrometer which measure electrons in 72 logarithmically spaced energy levels from 10 eV to 26.4 keV and has a polar angle resolution of $\Delta\theta = 15°$, with the option to increase the resolution on a single anode up to 3.75°. The geometric factor of each 15° polar angle sector of the spectrometer is equal to $6.0 \cdot 10^{-8}\,\mathrm{m^2\,sr}$, and the time step between energy levels is $T_{acc} = 3.9\,\mathrm{ms}$.

Based on Figure 1b, HEEA cannot reach the optimal range of energies for the measurement of the nonlinear perturbations. Therefore, we assumed a hypothetical extension of the HEEA energy range. Specifically, we chose to look

into an energy bin from 51.2 keV to 57.2 keV. We also increased T_{acc} to 15.6 ms, which is close to the time duration of the fourth subpacket (25 ms). In Fig. 2a we observe a region of a decreased phase space density at higher energies and pitch angles and a region of an increased phase space density at lower energies and pitch angles. The absolute decrease in phase space density is observed to reach about 4 % of the maximum PSD value of the hot electron distribution, which is about 10 % in relative numbers. Figure 2b shows the required particle counts, which are $10-20$ in the region corresponding to the phase space density decrease (the increased phase space density bump should decay in accordance with the quasilinear wave growth theory, which is not included in our non-selfconsistent simulation). Finally, Figure 2b also shows the $N_{C,exp}/N_{C,req}$ ratio. At pitch angle values where the decrease of the phase space density is most prominent, the ratio drops to 1, meaning that the observed density decrease would be equal to one standard deviation of the Poisson distribution. This shows that measurements from an improved HEEA instrument would be close to the bare limit of statistical significance.

4 Conclusion

We proved that with the instrumentation currently available on Cluster, a direct measurement of perturbations in electron velocity distributions due to the interaction with a chorus element is not possible, even if we assume an extended energy range and longer particle accumulation times. However, the estimated particle counts are close to the values required for statistically significant observations. With a dedicated experiment, an in situ observation of these perturbations should be within the current technical possibilities. Such an experiment would consist of electrostatic particle analyzers measuring electron energies up to 50 keV with a polar angle resolution about 5° or better, and with a geometric factor comparable to HEEA. During high chorus wave activity, the analyzer would operate in a fixed energy mode with accumulation times comparable to the theoretical time duration of a single subpacket. With this type of experiment, it should be possible to obtain direct confirmation of the processes described by the nonlinear growth theory of chorus rising tone emissions.

5 Acknowledgements

TODO M. Hanzelka, I. Kolmasova and O. Santolik acknowledge the support from the MEYS grant LTAUSA17070. M. Hanzelka and O. Santolik acknowledge support from Charles University through the GA UK project No. 64120.

References

[1] B. T. Tsurutani and E. J. Smith, "Postmidnight chorus: A substorm phenomenon," *J. Geophys. Res.*, vol. 79, no. 1, pp. 118–127, Jan. 1974.

[2] R. B. Horne, "Plasma astrophysics: Acceleration of killer electrons," *Nature Phys*, vol. 3, no. 9, pp. 590–591, Sep. 2007.

[3] W. Li, R. M. Thorne, Y. Nishimura, J. Bortnik, V. Angelopoulos *et al.*, "THEMIS analysis of observed equatorial electron distributions responsible for the chorus excitation," *J. Geophys. Res. Space Physics*, vol. 115, p. A00F11, Jun. 2010.

[4] O. Santolík, E. Macúšová, I. Kolmašová, N. Cornilleau-Wehrlin, and Y. Conchy, "Propagation of lower-band whistler-mode waves in the outer Van Allen belt: Systematic analysis of 11 years of multi-component data from the Cluster spacecraft," *Geophys. Res. Lett.*, vol. 41, pp. 2729–2737, Apr. 2014.

[5] A. G. Demekhov, U. Taubenschuss, M. Hanzelka, and O. Santolík, "Frequency Dependence of Very Low Frequency Chorus Poynting Flux in the Source Region: THEMIS Observations and a Model," *Geophys. Res. Lett.*, vol. 47, no. 6, p. e86958, Mar. 2020.

[6] O. Santolík, C. A. Kletzing, W. S. Kurth, G. B. Hospodarsky, and S. R. Bounds, "Fine structure of large-amplitude chorus wave packets," *Geophys. Res. Lett.*, vol. 41, pp. 293–299, Jan. 2014.

[7] D. Nunn, "A self-consistent theory of triggered VLF emissions," *Planet. Space Sci.*, vol. 22, no. 3, pp. 349–378, Mar. 1974.

[8] D. Summers, Y. Omura, Y. Miyashita, and D.-H. Lee, "Nonlinear spatiotemporal evolution of whistler mode chorus waves in Earth's inner magnetosphere," *J. Geophys. Res. Space Physics*, vol. 117, no. A9, p. A09206, Sep. 2012.

[9] A. G. Demekhov, "Generation of VLF emissions with the increasing and decreasing frequency in the magnetosperic cyclotron maser in the backward wave oscillator regime," *Radiophys. and Quantum Electron.*, vol. 53, no. 11, pp. 609–622, Apr. 2011.

[10] M. Hanzelka, O. Santolík, Y. Omura, I. Kolmašová, and C. A. Kletzing, "A Model of the Subpacket Structure of Rising Tone Chorus Emissions," *J. Geophys. Res. Space Physics*, vol. 125, no. 8, p. e28094, Aug. 2020.

[11] M. Hikishima, S. Yagitani, Y. Omura, and I. Nagano, "Full particle simulation of whistler-mode rising chorus emissions in the magnetosphere," *J. Geophys. Res. Space Physics*, vol. 114, p. A01203, Jan. 2009.

[12] A. D. Johnstone, C. Alsop, S. Burge, P. J. Carter, A. J. Coates *et al.*, "Peace: a Plasma Electron and Current Experiment," *Space Sci. Rev.*, vol. 79, pp. 351–398, Jan. 1997.